J. Biochem. 2010;148(2):189–200 doi:10.1093/jb/mvq050

JB THE JOURNAL OF BIOCHEMISTRY

Molecular characterization and expression pattern of four chemosensory proteins from diamondback moth, *Plutella xylostella* (Lepidoptera: Plutellidae)

Received April 16, 2010; accepted May 6, 2010; published online May 21, 2010

Xiaolei Liu, Qian Luo, Guohua Zhong, Muhammad Rizwan-ul-Haq and Meiying Hu*

Laboratory of Insect Toxicology and Key Laboratory of Natural Pesticide and Chemical Biology, Ministry of Education of China, South China Agricultural University, Guangzhou 510642, China

*Meiying Hu, Laboratory of Insect Toxicology and Key Laboratory of Natural Pesticide and Chemical Biology, Ministry of Education of China, South China Agricultural University, Wushan Road, Guangzhou 510642, China. Tel./Fax: +86 20 85280308, email: humy@scau.edu.cn

Some chemosensory proteins (CSPs) expressed in insect sensory appendages are thought to be involved in chemical signaling in moths. We cloned and characterized four CSP genes from *Plutella xylostella*. The deduced amino acid sequences of PxylCSP1, PxylCSP2, PxylCSP3 and PxylCSP4 revealed open reading frames of 152, 128, 126 and 126 amino acids, respectively, with four conserved cysteine residues. The expression patterns of the four PxylCSP genes were further investigated by reverse transcription (RT) PCR and real-time PCR. *PxylCSP1* and *PxylCSP2* genes were expressed in all the tested tissues with the highest expression level in the antennae and heads (without antennae) whereas *PxylCSP3* and *PxylCSP4* mRNA were distributed extensively in all the tested tissues without apparent quantitative differences. The transcription levels of these CSP genes depended on sex, age, mating and the genes. Fluorescence quenching with Rhodojaponin-III (R-III) and homology modelling studies indicated that PxylCSP1 was able to bind non-volatile oviposition deterrents, such as R-III. These ubiquitous proteins might have the role of extracting non-volatile compounds (oviposition deterrents or antifeedants) dispersed in the environment and transporting them to their receptor.

Keywords: *Plutella xylostella*/chemosensory proteins/expression pattern/binding property.

Abbreviations: CSPs, chemosensory proteins; PxylCSPs, *Plutella xylostella* CSPs; OBPs, odorant binding proteins; PBPs, pheromone binding proteins; CIP, calf intestinal phosphatase; TAP, tobacco acid pyrophosphatase; EDTA, ethylenediaminetetraacetic acid; PCR, polymerase chain reaction; GSP, gene-specific primer; OS-D, olfactory specific-protein type D; 5′ RACE, 5′ rapid amplification of 5′ cDNA ends; 3′ RACE, 3′ rapid amplification of 3′ cDNA ends; R-III, Rhodojaponin-III.

Two different soluble protein groups have been identified in the antennal lymph of insects. The first group comprises the odorant binding proteins (OBPs) (*1*–*3*); while the second group is formed by chemosensory proteins (CSPs) (*4*). A class of putative general CSPs has gained increasing interest over the last few years, expanding our understanding of the complexity of the repertoire of sensory binding proteins. The first CSP was found in *Drosophila melanogaster* and called OS-D (olfactory specific-protein type D) or A10 (*5*, *6*). Since then, many CSPs have been identified in several insect species (*4*, *7*–*17*), and in each case, different CSPs are encoded by distinct loci. In *Bombyx mori*, a DIG-RNA probe encoding the *BmorCSP1* hybridized not only with mRNAs from male and female antennae but also with mRNAs from legs and other parts of the insect body. Northern blot analysis revealed that *BmorCSP2* showed a very similar distribution pattern with no tissue specificity (*11*), like the three CSPs of *Heliothis virescens* that showed high levels of expression in legs (*10*, *12*). The CSP of *Cactoblastis cactorum* was as a cDNA from labial palps (*18*). The CSPs of *Mamestra hrassicae* were isolated as cDNAs from antennae and pheromone glands while as proteins (N-terminal sequences) from antennae, proboscis and legs (*13*, *18*, *19*). There are a lot of differences between CSPs and odorant binding proteins (OBPs) in tissue distribution and developmental expression, indicating that the roles of these proteins in chemoreception may also be different. Those results also suggest that CSPs may have functions in more systems not only in the olfaction and taste as general molecule carriers especially in the transport of contact sensory molecules.

Rhodojaponin-III (R-III), a grayanoid diterpene compound isolated from *Rhododendron molle* G. Don flowers, has been determined under laboratory and field conditions as an oviposition deterrent, antifeedant, stomach poison, contact toxicant and insect growth inhibitor against more than 40 species of agricultural pests (*20*–*23*). However, detailed studies of the mode of action and the target protein of oviposition deterrent of R-III are rare, rather small.

The diamondback moth, *Plutella xylostella* (Lepidoptera: Plutellidae) is an important agricultural pest throughout the world. The investigations about CSPs from *P. xylostella* (PxylCSPs) should have important impacts not only in fundamental genetics underlying chemosensation and olfaction but also in the control of the sensory abilities of insect pests through CSP expression. In the present study, we

report four PxylCSPs about their tissue distribution patterns as well as relative expression levels in male and female by using polymerase chain reaction (PCR) strategies. We also compare the PxylCSPs with previously reported sequences from other species of the Lepidoptera, and describe on the ligand-binding property of recombinantly expressed PxylCSP1, using fluorescence spectroscopy as well as homology modelling.

Materials and Methods

Insect rearing and tissue collection

Plutella xylostella larvae were fed with Chinese cabbage, *Brassica oleracea var. capitata* L. (Brassicaceae) and reared in the laboratory under the conditions as: 24 (±2)°C, 60 (±2)% relative humidity and 16 : 8 L : D photoperiod until pupation. Sexed pupae were kept inside Petri dishes in an environmental chamber at 24 (±2)°C, 60 (±2)% relative humidity and 16 : 8 L : D photoperiod until the moths emerged. Emerged moths were fed on 10% honey solution in culture cages (40 × 50 × 60 cm) at 24 (±2)°C, 60 (±2)% relative humidity and 16 : 8 L : D photoperiod. To obtain mated females, newly emerged male and female moths were paired individually in culture cages and allowed to mate.

Reverse transcription (RT)–PCR was performed by using the RNA isolated from, antennae, head (without antennae), thorax, abdomen, wing and legs from 3-day-old male and female moths. Real-time PCR was performed by using the RNA isolated from, 100 first-instar larvae, 50 second- and third-instar larvae, 20 fourth-instar larvae, 20 male, female pupae and antennae of 0, 5, 10 and 24 h-old-adult (virgin and mated) moths. To obtain mated moths, newly emerged male and female were paired individually in culture cages and allowed to mate and collected after 24 and 48 h. They were excised at the base and immediately transferred into eppendorf tubes immersed in liquid nitrogen. The same procedure was used for collecting head (without antennae), thorax, abdomen, wing and legs. All tissues were stored at −75°C until used experimentally.

Nucleic acid manipulation

Total RNA was extracted from the homogenized antennae or other tissues by using the E.Z.N.A.™ total RNA isolation system kit (Omega Bio-tech, Doraville, GA, USA) following the manufacturer's instructions. Total RNA was transcribed to single-strand cDNA that served as templates for PCR amplification by extension of an oligo$(dT)_{18}$ primer with MMLV reverse transcriptase (TaKaRa, Dalian, China) at 42°C for 60 min. The reaction was stopped by heating at 95°C for 5 min.

Genomic DNA was prepared from 3-day-old moths. The adults were grinded in liquid nitrogen and homogenized with 300 µl DNA extraction buffer [(100 mM Tris–HCl, pH 8.0; 50 mM ethylenediaminetetraacetic acid (EDTA); 200 mM NaCl; 1% sodium dodecyl sulfate (SDS)]. The homogenate was transferred to an eppendorf tube, gently mixed with 20 µl Proteinase K (20 mg/ml), incubated at 56°C for 3 h and centrifuged for 10 min at 12,000 *g*. The supernatant was transferred to a new tube, and DNA was extracted from it with an equal volume of phenol: chloroform : isoamyl alcohol (25 : 24 : 1) followed by an equal volume of chloroform : isoamyl alcohol (24 : 1). Each time, the sample was centrifuged for 5 min at 12,000 *g* to collect the aqueous phases. Two-and-a-half volumes of chilled ethanol were added to the aqueous supernatant for DNA precipitation. The pellets were washed in 70% ethanol, briefly vacuum-dried and DNA was redissolved in 50 µl TE buffer (10 mM Tris–HCl, pH 8.0; 1 mM EDTA, pH 8.0; 100 µg/ml RNase A).

Molecular cloning and sequencing

The cDNAs that encode CSPs of *P. xylostella* were amplified from antennal cDNA of moths. Nucleotide and deduced amino acid sequences of CSPs gene from several insects available in The National Center for Biotechnology Information (NCBI) were aligned. The conserved regions from the alignment were determined and the degenerate primers (3RCSP1, 3RCSP2, 3RCSP3 and 3RCSP4) were developed (Table I). Rapid amplification of cDNA ends (3′ RACE) PCR reactions were conducted on 3 µl of *P. xylostella* cDNA, with sense primers following 3′ RACE outer and inner PCR amplifications of *PxylCSP1* and *PxylCSP2* (3RCSP1 as *PxylCSP1, 2* 3′ RACE outer primer and 3RCSP2 as *PxylCSP1, 2* 3′ RACE inner primer); *PxylCSP3* and *PxylCSP4* (3RCSP3 as *PxylCSP3, 4* 3′ RACE outer primer and 3RCSP4 as *PxylCSP3, 4* 3′ RACE inner primer) with an antisense primer [oligo$(dT)_{20}$]. The reaction was performed in 50 µl with 3 µl single-stranded cDNA, 2.0 mM $MgCl_2$, 0.2 mM dNTP, 1.5 µM of each primer and 2.5 U Taq polymerase (TaKaRa). 3′ RACE outer PCR was preformed under the following conditions: 95°C for 3 min, followed by nine cycles at 94°C for 50 s, 65°C for 1 min and 72°C for 1 min, with a decrease of the annealing temperature by 1°C per cycle; 30 cycles at 94°C for 45 s, 56°C for 1 min and 72°C for 1 min; 72°C for 10 min before incubation at 4°C, and 3′ RACE inner PCR was preformed in the following conditions: 95°C for 3 min, followed by nine cycles at 94°C for 50 s, 65°C for 1 min and 72°C for 1 min, with a decrease of the annealing temperature by 1°C per cycle; 30 cycles at 94°C for 45 s, 58°C for 1 min and 72°C for 1 min; 72°C for 10 min before incubation at 4°C. Amplifications were successfully carried out in a MyCycler (Bio-Rad Laboratories Inc., Hercules, CA, USA).

5′ RACE of *P. xylostella* cDNA was performed by using the GeneRacer system (Invitrogen Life Technologies, Paisley, UK) following the manufacturer's instructions. In contrast to conventional 5′ RACE, the GeneRacer system ensures that only mature capped mRNA transcripts participate in the reaction. In brief, total RNA extracted from antennae was treated with calf intestinal phosphatase (CIP) to dephosphorylate the 5′ ends of truncated mRNA and non-mRNA molecules and thereby inhibit their participation in downstream reactions. The dephosphorylated RNA was treated with tobacco acid pyrophosphatase (TAP) to remove the 5′ cap structure from mature full-length mRNA, leaving a 5′ phosphate group available. A kit-supplied RNA oligonucleotide (5′-CGA CUG GAG CAC GAG GAC ACU GAC AUG GAC UGA AGG AGU AGA AA-3′) was ligated to the decapped mRNA by using T4 RNA ligase, thus providing a priming site for later amplification procedures. First-strand cDNA synthesis was performed by using SuperScript II reverse transcriptase and a kit-supplied oligo dT primer [5′-GCT GTC AAC GAT ACG CTA CGT AAC GGC ATG ACA GTG $(T)_{18}$-3′]. Double-stranded cDNA was subsequently prepared by amplifying the first-strand product using a reverse gene-specific primer (GSP) designed to be within the M2 receptor gene coding region and the GeneRacer 5′ primer (homologous to the previously ligated RNA oligonucleotide). A second nested PCR was performed by using a kit-supplied 5′ nested primer and a reverse nested GSP (see Table I for primer details). This step increased the product yield available for later cloning and eliminated any potential non-specific products of the first PCR. The nested PCR products were gel-purified and cloned as described below.

Regions of the CSP genes were amplified from genomic DNA by PCR to ascertain exon/intron structure of the genes. Specific primer pairs (Table I) were chosen for amplification. For PxylCSPs, the reactions were: 94°C for 3 min; 40 cycles at 94°C for 50 s, 50–64°C for 50 s, and 72°C for 2 min followed by incubation for 10 min at 72°C. LA Taq polymerase (TaKaRa) was used following the manufacturer's instructions.

PCR products were analysed by 1.5% agarose-gel electrophoresis, and purified by Agarose Gel DNA purification kit (TaKaRa). Purified products were subcloned into pGEM-T vector system (Takara) following the manufacturer's instructions. Plasmid DNA was transformed into DH5α-competent cells. Positive clones (based on restriction enzyme cleavage sites and PCR amplification) were sequenced by an ABI 377 automated sequencer (Applied Biosystems, Foster City, CA, USA).

Sequence analysis

DNA sequences were identified by NCBI-BLAST network server (*24*). The putative signal peptides and their cleavage sites were predicted by SignalP V 3.0 program (http://www.cbs.dtu.dk/services/SignalP/) (*25*). The hydrophobicity profile was determined by the method from Kyte and Doolittle (*26*). The sequence data were aligned and compared with Clustal X (1.81) (*27*). The phylogenetic tree was constructed with Neighbor Joining (NJ) by the MEGA3.1 program (*28*). Bootstrap analysis used 1,000 replications.

Table I. Oligonucleotide primers used for isolation and expression analysis of *P. xylostella* chemosensory proteins.

Primer name	Forward sequence (5′–3′)	Reverse sequence (5′–3′)	Purpose
3RCSP1	TACACNGAYAARTAYGHCAAYAT		3′ RACE first PCR
3RCSP2	TGCANTCCYGANGNYAAGGA		3′ RACE nested PCR
3RCSP3	YACNGAYAARTAYGACAAYATGGATC		3′ RACE first PCR
3RCSP4	CAARTAGGAYAAYATHGATCTNGACG		3′ RACE nested PCR
5P1		TTTATTTCTCTTCGCCATCGCCTTTCG	5′ RACE first PCR
5P1nest		ATTCGGCCTGTACTCGATGATGTAGCC	5′ RACE nested PCR
5P2		CGACTACGCTTTACACCAGCCAGCAACA	5′ RACE first PCR
5P2nest		GAGGCCTTGACCTCCTTGAGTTCCTTCT	5′ RACE nested PCR
5P3		TGTATTTCCCGGCGGGGTCGTACTTGT	5′ RACE first PCR
5P3nest		CGATCACCTTCCTCACGGCTGGCTTCTG	5′ RACE nested PCR
5P4		AAGCGTCAGTTTGGTTCAGAAATCAGC	5′ RACE first PCR
5P4nest		TACTCTCCCTTGGGGTCCTTCTTGCT	5′ RACE nested PCR
GeneRacer 5′ Primer	CGACTGGAGCACGAGGACACTGA		5′ RACE first PCR
GeneRacer 5′ Nested Primer	GGACACTGACATGGACTGAAGGAGA		5′ RACE nested PCR
PlxyCSP1	ATGAAGTCAGCGGCATTCATCGCACTGT	TTATTTCTCTTCGCCATCGCCTTTCG	Genomic DNA isolation
PlxyCSP2	ATGCAGAAGCTAACCCTGGCTTGTCTCC	TACACCAGCCAGCAACATGAGGCCTTG	Genomic DNA isolation
PlxyCSP3	ATGAACTCCTTGGTACTAGTATGCCTTG	TACGCCTTGACAGCGCGCAGTTGGTCC	Genomic DNA isolation
PlxyCSP4	ATGCAGACCGTGACTCTCCTATGCCTGT	TTAATCAGATCCTTCGAGGAACTTGGCG	Genomic DNA isolation
PlxyCSP1-RT	ATGAAGTCAGCGGCATTCATCGCACTGT	TTATTTCTCTTCGCCATCGCCTTTCG	RT–PCR
PlxyCSP2-RT	GCGCTGGAGAACAACTGCGGCAAATGC	AGACTACGCTTTACACCAGCCAGCAACA	RT–PCR
PlxyCSP3-RT	GAACGTGGACGAGATCCTGGCTAATG	TGGTCCTCGTACTGGGCGGTGTATTTC	RT–PCR
PlxyCSP4-RT	GTGCAGGGCCCCTTGCTCAGGAAGCACT	CTGGTGCGAGTCGTGGTGAAGGGCT	RT–PCR
PlxyActin-RT	GCGACTTGACCGACTACC	GGAATGAGGGCTGGAACA	RT–PCR
PlxyCSP1-RealT	CGGGAAGGAGCTAAAACATACTCT	TCTGCGTACATTTGCGACAGT	Real-time PCR
PlxyCSP2-RealT	CCCCAACGACTCCCACTACA	GCACTTCACATACGGCACCA	Real-time PCR
PlxyCSP3-RealT	GGCTAAGGAACTCAAATCTCACATC	CTGTTTGTCCGTGCATTTGG	Real-time PCR
PlxyCSP4-RealT	CGACTTTAAGAGAGTGATCCCAGAA	CGGCAGTTGCTCCTGGAA	Real-time PCR
PlxyActin-RealT	GCGACTTGACCGACTACC	GGAATGAGGGCTGGAACA	Real-time PCR

Distribution pattern of PxylCSPs expression

Tissue localization of expression of PxylCSPs was assessed by RT–PCR with the cDNA templates from antennae and other tissues of male and female moths. Specific primer pairs (Table I) were derived from the cDNA sequences, spanning at least one predicted intron region, thus allowing us to distinguish genomic contaminants in the cDNA preparation. For testing the integrity of the cDNA templates, a control primer pair (Table I) from the coding region of the *P. xylostella Actin* gene (GenBank AB282645) was used. PCR began at 94°C for 3 min, then five cycles at 95°C for 50 s, 54°C for 50 s and 72°C for 1 min (with a decrease of the annealing temperature by 1°C per cycle); followed by 35 cycles at 95°C for 50 s, 54°C for 1 min and 72°C for 1 min; with a final 10 min incubation at 72°C. PCR products were analysed on 1.5% agarose gels.

Expression profiling of PxylCSPs based on real-time PCR

Real-time PCR was performed in an iCycler iQ Real-Time PCR Detection System (Bio-Rad) with SYBR green dye bound to double-strand DNA at the end of each elongation cycle (Taraka). Each pair of PCR primers was designed to span a cDNA exon–exon border to avoid amplification of potential traces of genomic DNA (*29*). The primers of *PxylCSP1*, *PxylCSP2*, *PxylCSP3* and *PxylCSP4* (Table I) amplified 64, 94, 69 and 111 bp fragments from cDNA, respectively. As an endogenous control to normalize the results of a variable target gene and to correct for sample-to-sample variation, the amplification size of *Actin* gene primers (Table I) was 252 bp.

Real-time PCR was conducted in 25 µl reactions that contained 12.5 µl of 2× SYBR Green PCR Master Mix, 0.5 µl of each primer (10 µM), 2.5 µl of sample cDNA and 9 µl sterilized ultrapure H_2O (Millipore). To check reproducibility, test samples, endogenous control and 'no sample control' were done in triplicate. Cycling parameters included 94°C for 2 min, 41 cycles at 94°C for 30 s and 64.5°C for 45 s. The products were analysed by sequencing, agarose gel electrophoresis and performing a melting curve, which indicated that each reaction did not produce non-specific amplification.

Relative quantification was performed by using the comparative $2^{-\Delta\Delta CT}$ method (*30*) to identify the amount of CSP mRNA in larvae, pupae and adults. All data were normalized to endogenous *Actin* levels from the same individual sample. In the analysis of the relative fold-change, the first-instar larvae sample, which was one of the experimental samples, was taken as the calibrator (*31*). Thus, the relative fold-change was assessed by comparing the expression level of *PxylCSPs* in other developmental stages to that in first instar.

For a valid $\Delta\Delta C_T$ calculation with the comparative $2^{-\Delta\Delta CT}$ method for relative quantification, the amplification efficiencies of the target and reference must be approximately equal. To confirm this, a pilot experiment was conducted to look at how ΔC_T ($C_{T,\ Target} - C_{T,\ Actin}$) varies with template dilution. Briefly, four serial 10-fold dilutions of cDNA from each sample were amplified. For each dilution, amplifications were performed in triplicate with primers for CSP and actin. The average C_T was calculated for both CSP and actin then the ΔC_T was determined. A plot of the log cDNA dilution versus ΔC_T was made (fluorescence versus cycle of real-time PCR and standard curve in Supplementary Figs 1 and 2). Data were analysed by ANOVA and regression analysis using the Statistical Analysis System (SAS) 8.01, 2000 software. ANOVA was carried out using Tukey's HSD tests at $P < 0.05$ to examine specific differences between groups (Supplementary Table 1).

Recombinant PxylCSP1

cDNA derived from *P. xylostella* antennae, containing the *PxylCSP1* gene, was amplified by PCR with the following primers: forward, 5′-CTGCTACATATGGAAGACAAGCCAACT; and reverse, 5′-CCGCTCGAGTTATTTCTCTTCGCCATCGC. The primers introduced an Nde I restriction site in the forward primer and an Xho I restriction site in the reverse primer. The PCR product was cloned into pCR-blunt-II^{TM} (Invitrogen, Carlsbad, CA, USA). The gene was then moved into pET-21a and used to transform BL21 (λDE3) *Escherichia coli* cells. Expression was induced overnight at 28°C in lactose-containing Luria–Bertani medium. The cell pellet was extracted with *t*-butanol/water and the aqueous phase was precipitated with 0.5 M ammonium sulphate. The supernatant was dialysed and applied to a DE52 column. The 0.35 M NaCl eluent was applied to a phenyl sepharose column in 0.5 M ammonium sulphate and eluted with 20 mM Tris, pH 8.4. A final purification step was carried out on a Superdex-75 column (GE Healthcare, Piscataway, NJ, USA) in 0.02 M Tris, pH 7.2, 0.1 M NaCl.

Western immunoblotting

Briefly, SDS–PAGE resolved protein bands were transferred to polyvinylidine fluoride (PVDF) membranes (Millipore, Bedford, MA, USA) using liquid transfer system. After transfer, the membranes were blocked with 5% non-fat milk in PBST buffer (PBS plus 0.05% Tween 20, pH 7.4) and incubated with rabbit primary antiserum against PxylCSP1 (the antiserum was prepared by our laboratory) in PBST at an antibody dilution of 1 : 2,000 for 2 h. After several washes with PBST, horseradish peroxidase (HRP)-conjugated goat anti-rabbit IgG as secondary antibody was applied for 2 h, whereas 3,3′,5,5′-tetramethylbenzidine (TMB) was used as staining substrate.

Fluorescence spectroscopy

R-III (2,3-epoxy-5,6,10,14,16-grayanotoxanepentol) was prepared from *R. molle* flowers collected from Qujiang County, Guangdong Province, South China, using methods described by Zhong *et al.* (*32*). The R-III had a purity of more than 95%. Methanolic solutions (100%) were freshly prepared. Fluorescence quenching was measured using a Cary Eclipse (Varian). Fluorescence measurements were made in a right angle configuration at 23°C by using 5-nm excitation and 5-nm emission bandwidths. The excitation wavelength was 295 nm and the emission spectra were measured between 250 and 550 nm. In all experiments the final methanol concentration in the cuvette was kept below 1%. Samples contained 1 μM protein in 10 mM Tris buffer, 25 mM NaCl, pH 8.0; ligand was used at concentrations between 0 and 300 μM.

In order to estimate the affinity of R-III to PxylCSP1, the fluorescence intensities at 318 nm at increasing concentrations of quencher were plotted versus the quencher concentration. The K_d values were estimated by non-linear regression using Prism 5.0 (GraphPad software Inc.).

Homology modelling and protein–ligand interaction

Homology modelling and protein–ligand interaction were carried out using the method as described by Zheng *et al.* (*33*) and Sun *et al.* (*34*). A three-dimensional (3D) model of the PxylCSP1 was generated based on the crystal structure of the chemosensory protein CSP-sg4 (SgreCSP4 code 2GVS) by using the Build Homology Models in Discovery studio 2.0. The final refined model was obtained and was further assessed by Profile-3D and Ramachandran Plot. With this model, an automated flexible docking was performed by using a combination of CHARMm type and simulated annealing procedures.

Results

Identification of cDNAs and genomic DNA sequences encoding P. xylostella CSPs

RT–PCR was performed with four degenerate primers identified four cDNA fragments of 300, 450, 350 and 360 bp, named *PxylCSP1*, *PxylCSP2*, *PxylCSP3* and *PxylCSP4*, respectively. A RACE procedure was further used to obtain full-length cDNA sequences of these four genes from *P. xylostella*. The sequences of *PxylCSP1*, *PxylCSP2*, *PxylCSP3* and *PxylCSP4* (Supplementary Fig. 3) were deposited in GenBank with accession number EF186791, EF196792, EF202828 and EF202829, respectively.

The isolated cDNA clone encoding PxylCSP1 was 668 bp and contained a 459 bp open reading frame encoded a polypeptide with 152 amino acids. The initial 17 amino acids were predicted as a signal peptide followed by polypeptide of 135 amino acids with a molecular mass of 15,466 Da and an isoelectric point 4.96. The isolated cDNA clone encoding PxylCSP2 (535 bp) comprised the complete CSP precursor consisting of 18-amino acid signal peptide followed by polypeptide of 110 amino acids with a molecular mass of 13,038 Da and an isoelectric point 6.38. The cDNA representing PxylCSP3 was 526 bp with 62 bp 5′ UTR and poly-A tail. The 381 bp open reading frame encoded a protein of 126 amino acids with the first 17 amino acids predicted to be a signal peptide followed by polypeptide of 109 amino acids with a molecular mass of 12,443 Da and an isoelectric point 9.08. The isolated cDNA clone encoding PxylCSP4 (864 bp) comprised the complete CSP precursor consisting of an 18-amino acid signal peptide followed by polypeptide of 109 amino acids with a molecular mass of 12,225 Da and an isoelectric point 8.33. That the four CSPs display similar hydropathy profiles (not shown) and the presence of putative signal sequences suggest that these proteins were secreted to the extracellular fluid. The identification of these four PxylCSPs added new members to the moth CSP family, and enabled future studies on structure–function relationship in CSPs, particularly with respect to their discriminating ability among different lipophilic components.

We aligned the polypeptide sequences of PxylCSP1, PxylCSP2, PxylCSP3 and PxylCSP4 with other Lepidopteran CSPs published on GenBank (Fig. 1). These four PxylCSPs have conserved characteristic for Lepidopteran CSPs, including hydrophobic domains, and four cysteine residues (positions C^{29}, C^{36}, C^{54}, C^{57}) that are believed to form two disulfide bridges. A phylogenetic tree was constructed using the protein sequences of Lepidopteran CSPs (Fig. 2). The cladogram indicated that PxylCSPs were divided into three groups (CSP 1, CSP 2 and CSP 3); PxylCSP2 and PxylCSP3 belonged to CSP 2. PxylCSP4 belonged to CSP3 and was similar to BmorCSP2. PxylCSP1 belonged to individual cluster and was found to be distant from the other CSPs. Similarity analysis of amino acid sequences of CSPs further confirmed the phylogenetic result. The four PxylCSPs showed only 30–55% identity, but were more identical to CSPs of the same cluster from other moth species. PxylCSP2 displayed high similarity with HvirCSP1 (72.8%), MbraCSPB2 (72.2%), MbraCSPB4 (72.2%) and MbraCSPB1 (69.4%), while PxylCSP3 was more identical to MbraCSPB1 (59.3%), MbraCSPB2 (57.4%) and MbraCSPB4 (57.4%). PxylCSP4 showed only 20–35% similarity to lepidopteran CSPs but 41.7% to BmorCSP2.

To understand exon/intron structure of genes, the four CSP genes were cloned and sequenced from genomic DNA. They all contained one intron having a similar exon/intron structure. The intron in *PxylCSP1*, *PxylCSP3* and *PxylCSP4* was located after codon for Lys46. However, the intron in *PxylCS*P2 was located after codon for Lys47 and the intron site sequence was AAGG/AG. The ends of the introns had a typical GT–AG structure (Supplementary Fig. 3).

Tissue distribution of expression

To further investigate the role of CSPs in moth chemosensory, RT–PCR experiments were performed by using specific primers to determine the tissue distribution of *PxylCSP1*, *PxylCSP2*, *PxylCSP3* and *PxylCSP4* (Fig. 3). RT–PCR products of the

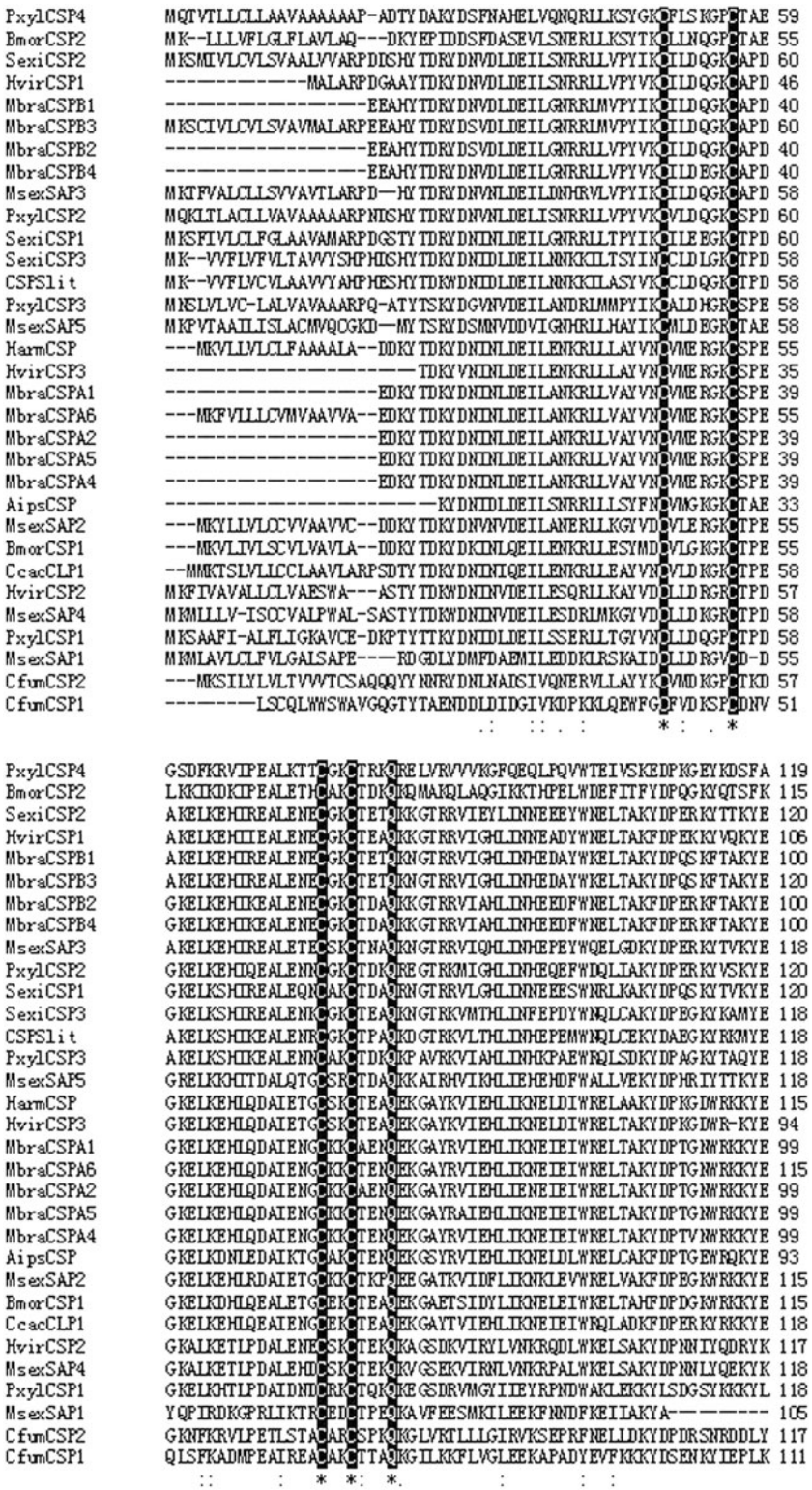

Fig. 1 Alignment of mature PxylCSP1, PxylCSP2, PxylCSP3 and PxylCSP4 from *P. xylostell* with their orthologs from other Lepidoptera. GenBank accession numbers—PxylCSP1 (*P. xylostell,* ABM67686), PxylCSP2 (*P. xylostell,* ABM67687), PxylCSP3 (*P. xylostell,* ABM92663), PxylCSP4 (*P. xylostell,* ABM92664), SexiCSP1 (*Spodoptera. exigua*, ABM67688), SexiCSP2 (*S. exigua*, ABM67689), SexiCSP3 (*S. exigua*, ABM67690), CSPSlit (*S. litura*, AAY26143), AipsCSP (*Agrotis ipsilon*, AAP57460), BmorCSP1 (*B. mori*, AAM34276), BmorCSP2 (*B. mori*, AAM34275), CcacCLP1 (*C. cactorum*, AAC47827), CfumCSP1 (*Choristoneura fumiferana*, AAR84077), CfumCSP2 (*C. fumiferana*, AAR84078), HarmCSP (*Helicoverpa armigera*, AAK53762), HvirCSP1 (*H. virescens*, AAM77041), HvirCSP2 (*H. virescens*, AAM77040), HvirCSP3 (*H. virescens*, AAM77042), MbraCSPA1 (*M. brassicae*, AAF19647), MbraCSPA2 (*M. brassicae*, AAF19648), MbraCSPA4 (*M. brassicae*, AAF19650), MbraCSPA5 (*M. brassicae*, AAF19651), MbraCSPA6 (*M. brassicae*, AAF71289), MbraCSPB1 (*M. brassicae*, AAF19652). MbraCSPB2 (*M. brassicae*, AAF19653), MbraCSPB3 (*M. brassicae*, AAF71290), MbraCSPB4 (*M. brassicae*, AAF71291), MsexSAP1 (*Manduca sexta*, AAF16696), MsexSAP2 (*M. sexta*, AAF16714), MsexSAP3 (*M. sexta*, AAF16707), MsexSAP4 (*M. sexta*, AAF16721) and MsexSAP5 (*M. sexta*, AAF16716). Conserved amino acids in all CSPs were shown in a black background. Positions of four conserved cysteine residues were indicated by asterisks.

predicted size were observed significantly in reactions with antennal cDNA of both sexes. *PxylCSP1* and *PxylCSP2* genes were expressed in all the tested tissues but the highest expression level was found to be in the antennae and heads (without antennae); *PxylCSP3* and *PxylCSP4* mRNA distributed extensively in all above-mentioned tissues, without apparent quantitative differences. The integrity of the cDNA templates prepared from different tissues was verified by primers specific for the actin gene. In all cDNA preparations, an *Actin* amplification product of the correct size was amplified.

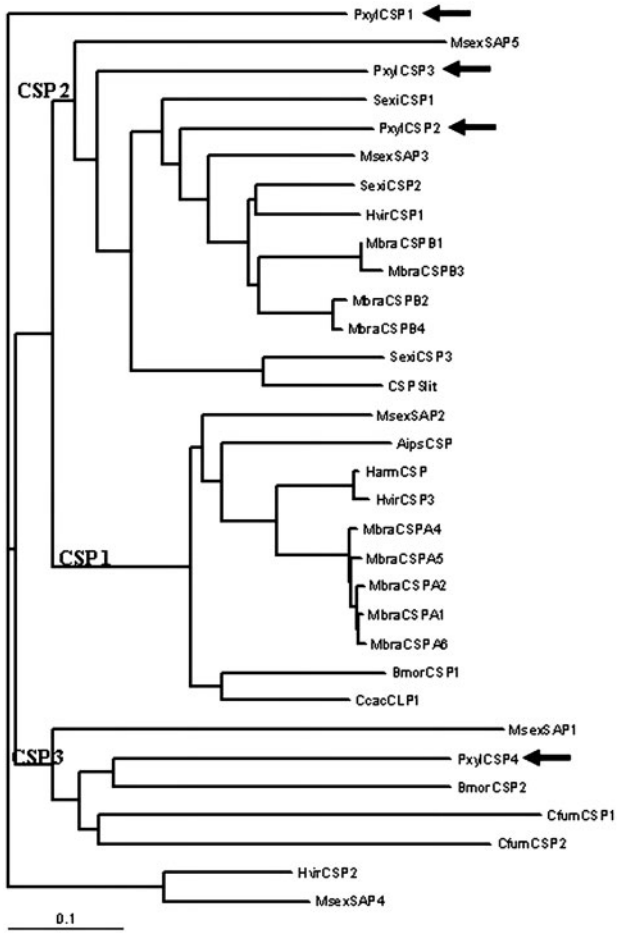

Fig. 2 Phylogenetic analysis based on PxylCSP1, PxylCSP2, PxylCSP3 and PxylCSP4 amino acid sequences. The tree was made by the neighbor-joining method with multiple alignments of amino acid sequences from Fig. 1. The CSPs from *P. xylostella* were indicated by arrows. Bootstrap analysis used 1,000 replications. The bar indicated phylogenetic distance value.

Temporal expression of PxylCSPs

Real-time PCR was performed to compare the transcript levels of *P. xylostella* CSPs from antennae of male to female moths and through a larval molt cycle. For each sex and each time, cDNA was synthesized from mRNA isolated from pools of 200 antennae. For sample analysis, the comparative $2^{-\Delta\Delta CT}$ method (*30*) was used to quantify the results obtained for PxylCSP transcripts by using real-time PCR. All samples were normalized with reference to *Actin*. The absolute values of the slope of all lines from template dilution plots (log cDNA dilution versus ΔC_T) were close to zero. Therefore, the efficiencies of the target and reference genes were similar in our analysis, and the $\Delta\Delta C_T$ calculation method was used for relative quantification.

PxylCSPs were expressed throughout the life cycle of *P. xylostella* (larva, pupae and adult) (Figs 4 and 5, Supplementary Table 1). The expression levels of both *PxylCSP1* and *PxylCSP2* were very low in larval and pupae stages compared with adult with only 1-fold increase (Figs 4A and B, and 5A and B), and the difference among the three stages was statistically significant (Supplementary Table 1). However, the transcription levels of both *PxylCSP3* and *PxylCSP4* were low in the life cycle of *P. xylostella* (Supplementary Table 1). The transcription levels of all *PxylCSP1*, *PxylCSP3* and *PxylCSP4* were the highest in first instar of whole larval period, and the transcription level of *PxylCSP1* was ~2.5–5 times that of other larval periods; the transcription level of *PxylCSP2* was ~2–3 times that of the other larval periods. However, the transcription levels of all *PxylCSP2*,

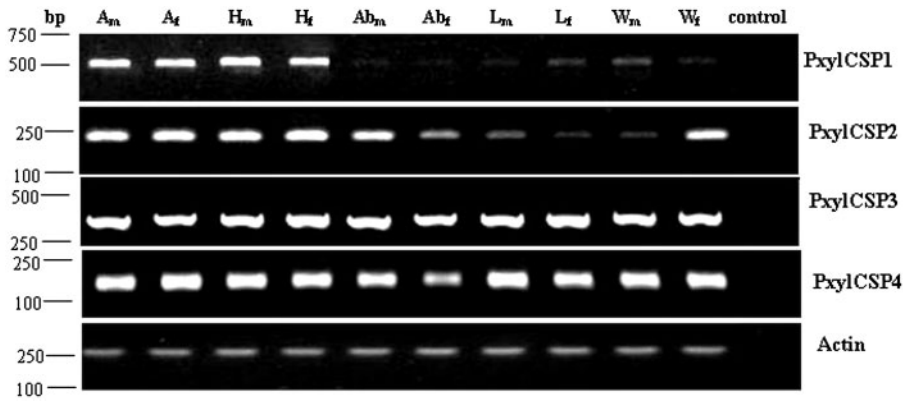

Fig. 3 Tissue-specific expression of *PxylCSPs*. RT–PCRs were performed by using RNAs isolated from the different tissues. Amplification products were analysed on agarose gels and visualized by UV illumination after staining with ethidium bromide. Based on the primer design, the sizes of the expected PCR products were 491 bp for *PxylCSP1*, 238 bp for *PxylCSP2*, 406 bp for *PxylCSP3*, 235 bp for *PxylCSP4* and 252 bp for *actin* (control). A_m: male antennae, A_f: female antennae, H_m: male head (without antennae), H_f: female head (without antennae), Ab_m: male abdomen, Ab_f: female abdomen, L_m: male leg, L_f: female leg, W_m: male wing, W_f: female wing, control: no-template (negative control) ensures the specificity of the amplifications. The position of molecular weight markers (bp) is indicated on the left side.

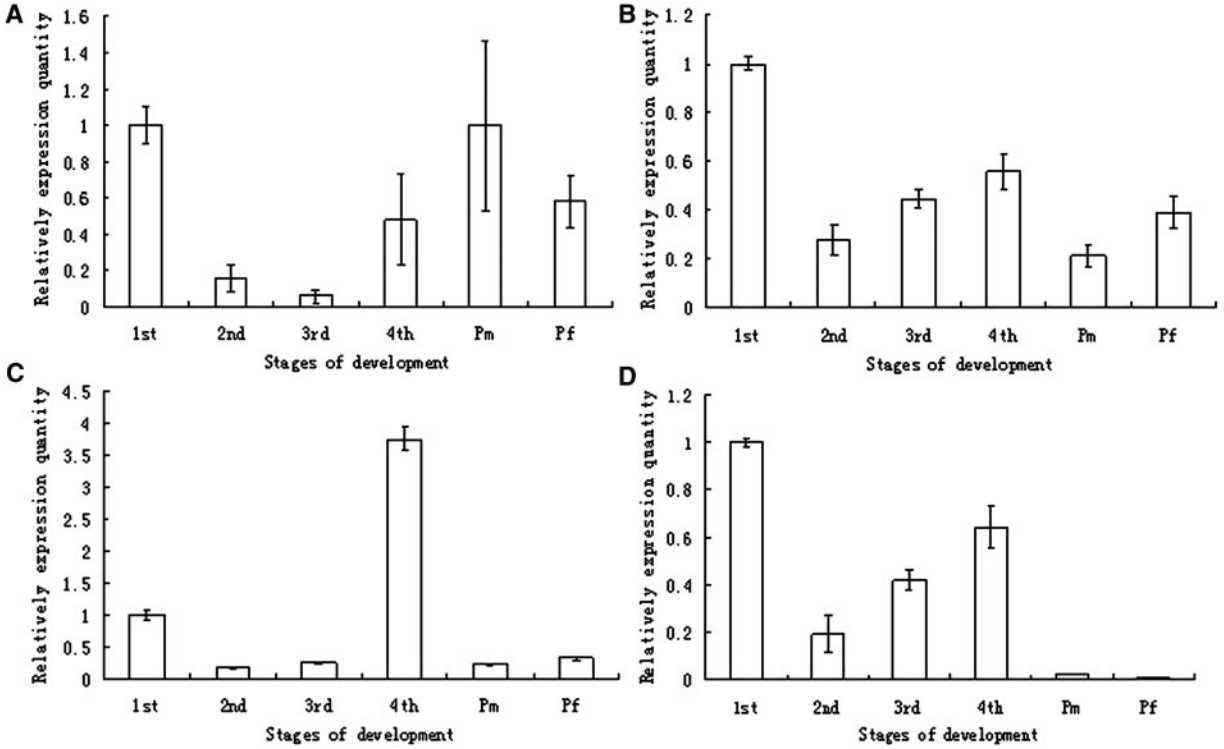

Fig. 4 Relative quantification of expression of *P. xylostella* CSPs amplified through a larval molt cycle by real-time PCR. *x*-axis shows developmental stages while *y*-axis shows the relative expression quantity (mean ± standard error of the mean), the expression of PxylCSPs in the first-instar larvae sample was taken as the calibrator. 1st: First-instar larvae, 2nd: second-instar larvae, 3rd: third-instar larvae, 4th: fourth-instar larvae, P_m: male pupae, P_f : female pupae. (A) *PxylCSP1* expression; (B) *PxylCSP2* expression; (C) *PxylCSP3* expression and (D) *PxylCSP4* expression.

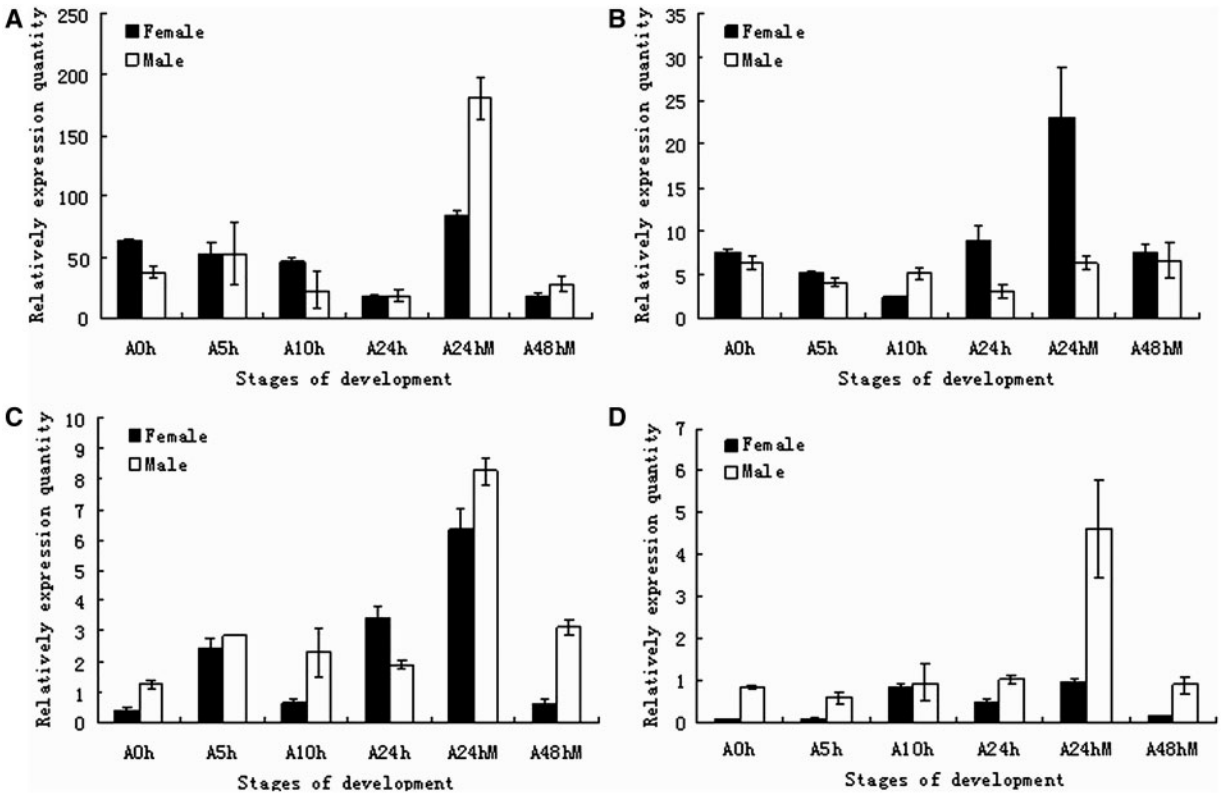

Fig. 5 Relative quantification of expression of *P. xylostella* CSPs amplified at separate times by real-time PCR. *x*-axis shows developmental stages while *y*-axis shows the relative expression quantity (mean ± standard error of the mean), the expression of PxylCSPs in the first-instar larvae sample was taken as the calibrator. A: antennae; 0, 5, 10 and 24 h refer to the adult at 0, 5, 10 and 24 h after eclosion; 24 and 48 h M refer to the adult at 24 and 48 h after mated. (A) *PxylCSP1* expression; (B) *PxylCSP2* expression; (C) *PxylCSP3* expression and (D) *PxylCSP4* expression.

PxylCSP3 and *PxylCSP4* (0.28 ± 0.06, 0.18 ± 0.02, 0.19 ± 0.08, respectively) were the lowest in second instar in comparison to complete larval period, with a continuous rising from second to fourth instar. The transcription levels of both *PxylCSP1* and *PxylCSP4* in male pupae were higher than that in female pupae, and there were no significant differences among them; on the contrary, the transcription levels of both *PxylCSP2* and *PxylCSP3* in female pupae were higher than that in male pupae, and no significant difference were found among them (Supplementary Table 1).

The expression levels of CSP genes after eclosion were shown in Fig. 5, Table II, and Supplementary Table 1. Mated individuals showed much higher levels of *PxylCSPs* expression at 24 h post-emergence than their unmated counterparts, but they showed lower levels of *PxylCSPs* expression at 48 h post-emergence; the relative quantification of expression of PxylCSPs had significant differences between mated and non-mated individuals at 24 h ($P < 0.05$) (Supplementary Table 1). The transcription levels of *PxylCSPs* in 5 h-old moth antennae were the lowest in males. The expression levels of *PxylCSP1*, *PxylCSP3* and *PxylCSP4* in 24 h-old mated male antennae were ~2, 10 and 5 times higher than that in 24 h-old mated female antennae, respectively; whereas the expression level of *PxylCSP2* in female antennae was 4.3 times higher than that in male antennae at 24 h after mating (Table II). These results suggest that these CSP genes play different roles in the adult development and diverse chemosensory tissues.

Recombinant PxylCSP1

Because the most abundant CSP in *P. xylostella* antennae was shown to bind to chemical signals, we reasoned that *PxylCSP1*, one of the most abundant CSP in *P. xylostella* antennae, may also be involved in chemical signaling selects and controls. Therefore, we expressed recombinant *PxylCSP1* in order to determine its ligand-binding properties. Transformed *E. coli* cells were induced to express PxylCSP1. Extraction from the cell pellet and purification (Fig. 6) typically yielded 20 ml of 50–100 μM PxylCSP1 per litre of medium. For some experiments, a final gel permeation step on a Superdex-75 column was included. The purified protein was resolved as a single band with molecular weight of 17 kDa by SDS–PAGE and verified by western blot using anti-PxylCSP1 antiboby (Fig. 6, lane 6).

Table II. Ratio of *P. xylostella* CSP gene expression levels in female compared with male antennae determined by real-time PCR.

	A0h	A5h	A10h	A24h	A24hM	A48hM
PlxyCSP1	1.414	2.868	2.479	0.493	0.473	0.664
PlxyCSP2	0.678	3.605	2.532	0.586	4.317	1.042
PlxyCSP3	0.895	0.841	0.297	1.670	0.104	0.172
PlxyCSP4	0.090	0.174	0.946	0.463	0.207	0.177

Fluorescence binding assays

In order to check whether R-III binds within the internal cavity of the PxylCSP1, we measured the influence of R-III on the CSP intrinsic fluorescence. In the presence of saturating concentrations of the compound, the intrinsic tryptophan fluorescence of PxylCSP1 was quenched at 59.1% (Fig. 7A), which suggests that the tryptophan interacts with the ligand. This decrease in fluorescence intensity was associated with a red shift of the emission maximum, from 318 to 335 nm with R-III, indicating that the tryptophan environment becomes probably more hydrophilic upon ligand binding. To determine the affinity of PxylCSP1 for the ligand, the fluorescence quenching at 318 nm was measured as a function of ligand concentration, and the dissociation constant was estimated by non-linear regression of the binding curve (Fig. 7A). The K_d value determined was 1.38 μM, respectively, in the range of values observed for PBP (Pheromone binding protein)-pheromone complexes (*35*, *36*).

Homology modelling and protein–ligand interaction

To understand the interaction between PxylCSP1 and R-III, the PxylCSP1–R-III (P–R) complex was generated using the Build Homology Models in Discovery studio and the binding 3D conformation of the P–R complex was shown in Fig. 7B. This figure showed that R-III located in the centre of the active site, and was stabilized by hydrogen bonding and hydrophobic interactions. Hydrogen bonds played an important role for structure and function of biological molecules. The hydrogen bond present in the P–R complex was shown in Fig. 7C. The H54 of R-III is tightly bound to the side-chain S of Met68 by a hydrogen bond. The hydrogen bonding interaction enhances the stability of the P–R complex.

To determine the key residues that comprise the active site of the model, the interaction energies of the ligand with each of the residues in the active site of PxylCSP1 were calculated. Significant binding-site residues in the models were identified by the total interaction energy between the ligand and each amino acid residues in the enzyme. This identification, compared

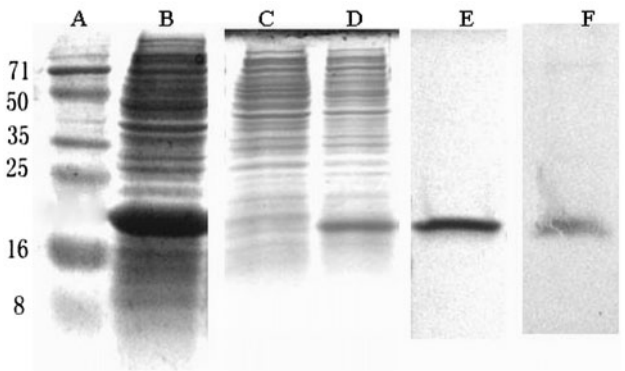

Fig. 6 Purification of *P. xylostella* chemosensory protein 1 (PxylCSP1) from *E. coli*. Lane A: molecular weight markers, kDa; B: whole cell extract; C: 0.2 M NaCl wash; D: 0.35 M NaCl wash; E: phenyl sepharose eluent; F: detection of purified CSP1 by western blot.

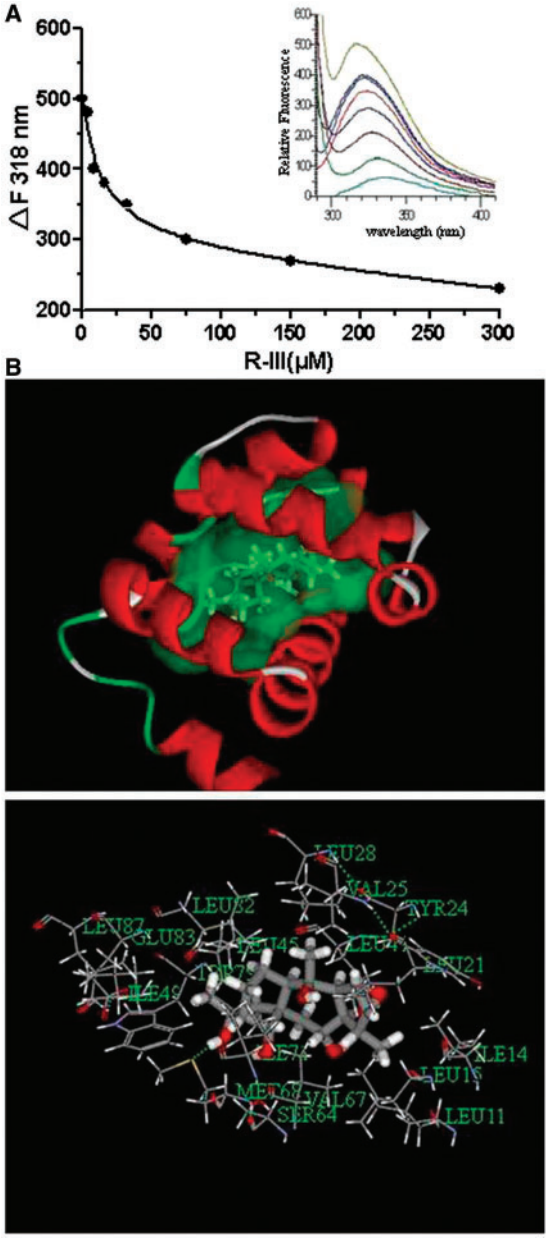

Fig. 7 Complex of PxylCSP1 with R-III. (A) Tryptophan fluorescence quenching curve with R-III. The tryptophan fluorescence intensities (corrected for dilution) at the emission maxima were plotted as a function of the quencher concentration. The quenching spectra obtained upon addition of R-III were shown in the insets. (B) Stereo picture of the 3D-structure of complex PxylCSP1–R-III. (C) The hydrogen bonding interaction of complex PxylCSP1–R-III. The modified key residues include Met68 and Val67.

with a definition based on the distance from the ligand, could clearly show the relative significance for every residue. Table III provides the interaction energies including the total, van der Waals and electrostatic energies with the total energies lower than −1.00 kcal mol^{-1} for all residues in the P–R complex. In Table III we could also see that the P–R complex had a favourable total interaction energy of −26.66 kcal mol^{-1}, the van der Waals and electrostatic energies were −24.25 and −2.44 kcal mol^{-1}, respectively. Through interaction analysis, we know that Met68, Val67, Tyr24, Leu21 and Leu28 were important anchoring residues for R-III and were the main contributors to the ligand interaction. For the hydrophobic residues of Met68, Val67, Tyr24, Leu21, Trp79 and Leu28, the interaction energies with R-III consisted mainly of van der Waals interactions. These results indicate that both the van der Waals and electrostatic energies are important for the P–R complex interaction.

Table III. The total energy (E_{total}), van der Waals energy (E_{vdw}) and electrostatic energy (E_{ele}) between R-III and individual residues ($E_{total} < -1.00$ kcal mol^{-1} listed in energy rank order).

Residue	E_{total} (kcal mol^{-1})	E_{vdw} (kcal mol^{-1})	E_{ele} (kcal mol^{-1})
Total	−26.66	−24.25	−2.44
Met68	−3.83	−2.64	−1.19
Val67	−3.74	−1.99	−1.75
Tyr24	−2.35	−2.71	0.35
Leu21	−2.27	−2.05	−0.22
Leu28	−2.08	−2.17	0.09
Ile71	−1.88	−2.14	0.26
Leu11	−1.80	−1.54	−0.26
Ile14	−1.71	−1.75	0.03
Leu45	−1.52	−1.50	−0.03
Val25	−1.53	−1.64	0.11
Glu83	−1.43	−0.37	−1.06
Leu41	−1.30	−1.61	0.31
Trp79	−1.22	−2.14	0.92

Discussion

In this study, CSPs are found not only in external sensory tissues, but also in external and internal non-sensory tissues organs, further suggesting that the proteins may have diverse functions. RT–PCR analysis using PxylCSPs showed a very ubiquitous expression in different tissues of adults as well as in different stages of *P. xylostella* life cycle. It is reported as well that three HvirCSPs showed high expression levels in legs (*10*, *12*). In locusts, CSPs were expressed in male and female from adult as well as fifth-instar larvae, and were found in many different tissues including antennae, legs, thorax, abdomen, head and legs (*11*). In *Periplaneta Americana*, the CSP p10 was expressed in legs and antennae (*12*, *37*). *Drosophila melanogaster* pherokines phk-2 and phk-3 (*38*) were upregulated after viral and septic infection, respectively, revealing that CSPs might be involved in immunoreaction. This hypothesis that CSPs may bear the function of transporting hydrophobic cuticular hydrocarbons had been supported by the ability of AOBP, an OS-D-like protein from *M. brassicae*, to bind vaccenyl acetate (*39*). Some data published by Ozaki *et al.* also showed that *Camponotus japonicus* CSP (CjapCSP) enabled nestmate recognition by solubilizing cuticular hydrocarbons (*40*). Thus, in various insect species, the expression of CSP occurs in many different tissues and developmental stages having differences between the expression of CSPs and OBPs. These results suggest that CSPs may have a broader function than OBPs, functioning in more systems than olfaction and taste.

The expression levels of four CSP genes from mated male and female *P. xylostella* showed significantly higher than that of unmated male and female moths at 24 h post-emergence, and recovered to near original levels at 48 h post-emergence. It is also reported that two GOBPs of *P. xylostella* showed much higher levels of expression in mated adult antennae at 16 h post-emergence than their unmated counterparts (*41*). This result was also concordant with the report that mated female *P. xylostella* were more responsive to three green leaf volatiles (GLVs) [namely, (*Z*)-3-hexenyl acetate, (*E*)-2-hexenal and (*Z*)-3-hexen-1-ol] from *Brassica oleracea* subsp. *capitata* L. than males or unmated female moths (*42*). Moreover, a similar upregulation of several CSPs before moulting had been reported in moth *C. fumiferana* (*43*) and fruit fly *D. melanogaster* (*15*). Together with the reported upregulation of a CSP in regenerating legs of cockroach (*37*, *44*), this finding suggests that some members of CSP family are involved in tissue formation and/or regeneration.

In addition, we have constructed a 3D model of PxylCSP1 using the the Build Homology Models in Discovery studio 2.0. After energy minimization and molecular dynamics simulations, this refined model structure is obtained. The final refined model was assessed further by Profile-3D and Ramachandran Plot, and the results show that this model is reliable. The stable structure is further used for docking of R-III. Through the docking studies, the model structures of the ligand–receptor complex were obtained. The docking results indicate that conserved amino-acid residues in PxylCSP1 play an important role in maintaining a functional conformation and are directly involved in donor substrate binding. The interaction of PxylCSP1 and R-III proposed in this study are useful for understanding the potential mechanisms of PxylCSP1 and the ligand. As is well known, hydrogen bonds play an important role for the structure and function of biological molecules. Met68 is important for strong hydrogen-bonding interaction with R-III. On the other hand, the results reported here lead to the proposal of Trp79, Leu28, Tyr24 and Leu21as key residues because they have strong van der Waals contacts with the ligand. In addition, as well as the others in Table III, these residues are suggested as candidates for further experimental studies of structure–function relationships.

The binding properties of PxylCSP1 and R-III studied using tryptophan fluorescence quenching show that the inner fluorescence of PxylCSP1 can be quenched by R-III and higher concentration of R-III decrease the fluorescence intensity. The results indicate that PxylCSP1 is able to bind R-III with good affinity and tryptophan (Trp79) is laid in binding site of PxylCSP1, this result is consistent with predicted by Discovery studio software, which is similar to that in the bSULT1A1 binding to CoA and the CSPMbraA6 binding to C15Br (*45*, *46*). Based on these results, we hypothesize its putative function as a lipophilic compound carrier, and the standpoint that CSPs is one of the target proteins of oviposition deterrent of R-III is proposed.

The genes underlying olfaction and general chemosensation are most likely under different evolutionary pressures that may act selectively through defined regulatory elements (*47*, *48*). Specific intron structures, like the intron of PxylCSPs, may be key targets for regulatory mechanisms that control the differential expression or loss of specific CSPs. In short, the *P. xylostella* CSPs represent a multifunctional gene family that participates in a range of cellular processes requiring lipophilic compounds. The biological significance of a particular CSP will depend on when and where its message is expressed, because their functional roles appear to be context-dependent. However, definite proof of their physiological function needs to be provided by additional experiments such as gene knockdown studies and site-directed mutagenesis.

Supplementary Data

Supplementary Data are available at *JB* Online.

Funding

National Natural Science Foundation of China (No. 30871660); Doctor Subject Foundation of the Ministry of Education of China (No. 20094404110019).

Conflict of interest

None declared.

References

1. Vogt, R.G. and Riddiford, L.M. (1981) Pheromone binding and inactivation by moth antennae. *Nature* **293**, 161–163
2. Vogt, R.G., Riddiford, L.M., and Prestwich, G.D. (1985) Kinetic properties of a sex pheromone-degrading enzyme: the sensillar esterase of *Antherea polyphemus*. *Proc. Natl Acad. Sci. USA* **82**, 8827–8831
3. Vogt, R.G. and Riddiford, L.M. (1986) *Pheromone Reception: A Kinetic Equilibrium*. (Payne, T.L., Birch, M.C., and Kennedy, C.E.J., eds.), pp. 201–208, Clarendon Press, Oxford, New York
4. Angeli, S., Ceron, F., Scaloni, A., Monteforti, G., Minnocci, A., Petacchi, R., Pelosi, P., and Ceron, F. (1999) Purification, structural characterization, cloning and immunocytochemical localization of chemoreception proteins from *Schistocerca gregaria*. *Eur. Biochem.* **262**, 745–754
5. Mckenna, M.P., Hekmat-Scafe, D.S., Gaines, P., and Carlson, J.R. (1994) Putative *Drosophila* pheromone-binding proteins expressed in a subregion of the olfactory system. *J. Biol. Chem.* **269**, 16340–16347
6. Pikielny, C.W., Hasan, G., Rouyer, F., and Rosbash, M. (1994) Members of a family of *Drosophila* putative odorant-binding proteins are expressed in different subsets of olfactory hairs. *Neuron* **12**, 35–49
7. Danty, E., Arnold, G., Burmester, T., Huet, J.C., Huet, D., Pernollet, J.C., and Masson, C. (1998) Identification and developmental profiles of hexamerins in antenna and hemolymph of the honeybee *Apis mellifera*. *Insect Biochem. Mol. Biol.* **28**, 387–399
8. Picimbon, J.F. and Leal, W.S. (1999) Olfactory soluble proteins of cockroaches. *Insect Biochem. Mol. Biol.* **29**, 973–978
9. Robertson, H.M., Martos, R., Sears, C.R., Todres, E.Z., Walden, K.K.O., and Nardi, J.B. (1999) Diversity of odourant binding proteins revealed by an expressed

sequence tag project on male *Manduca sexta* moth antennae. *Insect Mol. Biol.* **8**, 501–518
10. Picimbon, J.F., Dietrich, K., Breer, H., and Krieger, J. (2000) Chemosensory proteins of *Locusta migratoria* (Orthoptera, Acriididae). *Insect Biochem. Mol. Biol.* **30**, 233–241
11. Picimbon, J.F., Dietrich, K., Angeli, S., Scaloni, A., Krieger, J., Breer, H., and Pelosi, P. (2000) Purification and molecular cloning of chemosensory proteins from *Bombyx mori*. *Arch Insect Biochem. Physiol.* **44**, 120–129
12. Picimbon, J.F., Dietrich, K., Krieger, J., and Breer, H. (2001) Identity and expression pattern of chemosensory proteins in *Heliothis virescens* (Lepidoptera, Noctuidae). *Insect Biochem. Mol. Biol.* **31**, 1173–1181
13. Nagnan-Le Meillour, P., Cain, A.H., Jacquin-Joly, E., Francois, M.C., Ramashadran, S., Maida, R., and Steinbrecht, R.A. (2000) Chemosensory proteins from the proboscis of *Mamestra brassicae*. *Chem. Senses* **25**, 541–553
14. Calvello, M., Brandazza, A., Navarrini, A., Dani, F.R., Turillazzi, S., Felicioli, A., and Pelosi, P. (2005) Expression of odorant-binding proteins and chemosensory proteins in some *Hymenoptera*. *Insect Biochem. Mol. Biol.* **35**, 297–307
15. Forêt, S., Warmer, K.W., and Maleszka, R. (2007) Chemosensory proteins in the honey bee: Insights from the annotated genome, comparative analyses and expressional profiling. *Insect Biochem. Mol. Biol.* **37**, 19–28
16. González, D., Zhao, Q., McMahan, Velasquez, Haskins, W.E., Sponsel, V., Cassill, A., and and Renthal, R. (2009) The major antennal chemosensory protein of red imported fire ant workers. *Insect Mol. Biol* **18**, 395–404
17. Zhang, S., Zhang, Y.J., Su, H.H., Gao, X.W., and Guo, Y.Y. (2009) Identification and expression pattern of putative odorant-binding proteins and chemosensory proteins in antennae of the *Microplitis mediator* (Hymenoptera: Braconidae). *Chem. Senses* **34**, 503–512
18. Zhou, J.J., Kan, Y., Antoniw, J., Pickett, J.A., and Field, L.M. (2006) Genome and EST analyses and expression of a gene family with putative functions in insect chemoreception. *Chem. Senses* **31**, 453–465
19. Maleszka, R. and Stange, G. (1997) Molecular cloning by a novel approach, of a cDNA encoding a putative olfactory protein in the labial palps of the moth *Cactoblastis cactorum*. *Gene* **202**, 39–43
20. Klocke, J.A., Hu, M.Y., Chiu, S., and Kubo, I. (1991) Grayanoid diterpene insect antifeedants and insecticides from *Rhododendron molle*. *Phytochemistry* **30**, 1797–1800
21. Hu, M.Y., Klocke, J.A., Chiu, S., and Kubo, I. (1993) Response of 5 insect species to a Botanical Insecticide, Rhodojapionin-III. *J. Econ. Entomol.* **86**, 706–711
22. Zhong, G.H., Hu, M.Y., Weng, Q.F., Ma, A.Q., and Xu, W.S. (2001) Laboratory and field evaluations of extracts from *Rhododendron molle* flowers as insect growth regulator to imported cabbage worm, *Pieris rapae* L (Lepidoptera: Pieridae). *J. Appl. Entomol.* **125**, 563–567
23. Zhong, G.H., Liu, J.X., Weng, Q.F., Hu, M.Y., and Luo, J.J. (2006) Laboratory and field evaluations of rhodojaponin-III against the imported cabbage worm *Pieris rapae* (L.) (Lepidoptera: pieridae). *Pest Manag. Sci.* **62**, 976–981
24. Altschul, S.F., Gish, W., Miller, W., Myers, E., and Lipman, D.J. (1990) Basic local alignment search tool. *J. Mol. Biol.* **215**, 403–410
25. Bendtsen, J.D., Nielsen, H., Vonheijne, G., and Brunak, S. (2004) Improved prediction of signal peptides: SignalP 3.0. *J. Mol. Biol.* **340**, 783–795
26. Kyte, J. and Doolittle, R.F. (1982) A simple method for displaying the hydropathic character of a protein. *J. Mol. Biol.* **157**, 105–132
27. Thompson, J.D., Gibson, T.J., Plewniak, F., Jeanmougin, F., and Higgin, D.G. (1997) The Clustal X windows interface: flexible strategies for multiple sequence alignment aided by quality analysis tools. *Nucleic Acid Res.* **25**, 4876–4882
28. Kumar, S., Tamura, K., and Nei, M. (2004) MEGA3: Integrated software for molecular evolutionary genetics analysis and sequence alignment. *Brief Bioinform.* **5**, 150–163
29. Bohbot, J. and Vogt, R.G. (2005) Antennal expressed genes of the yellow fever mosquito (*Aedes aegypti* L.); characterization of odorant-binding protein 10 and takeout. *Insect Biochem. Mol. Biol.* **35**, 961–979
30. Livak, K,J. and Schmittgen, T.D. (2001) Analysis of relative gene expression data using real-time quantitative PCR and the $2^{-\Delta\Delta CT}$ method. *Methods* **25**, 402–408
31. Mittapalli, O., Wise, I.L., and Shukle, R.H. (2006) Characterization of a serine carboxypeptidase in the salivary glands and fat body of the orange wheat blossom midge, *Sitodiplosis mosellana* (Diptera: Cecidomyiidae). *Insect Biochem. Mol. Biol.* **36**, 154–160
32. Zhong, G.H., Hu, M.Y., Wei, X.Y., Weng, Q.F., Xie, J.J., Liu, J.X., and Wang, W.X. (2005) Two new grayanne diterpenoids from the flowers of *Rhododendron molle* with cytotoxic activity against *Spodoptera frugiperda* cell line. *J. Nat. Prod.* **68**, 924–926
33. Zheng, Q.C., Li, Z.S., Xiao, J.F., Sun, M., Zhang, Y., and Sun, C.C. (2005) Homology modeling and PAPS ligand (cofactor) binding study of bovine phenol sulfotransferase. *J. Mol. Model.* **11**, 97–104
34. Sun, M., Li, Z.S., Zhang, Y., Zheng, Q.C., and Sun, C.C. (2005) Homology modeling and docking study of cyclin-dependent kinase (CDK) 10. *Bioorg. Med. Chem. Lett.* **15**, 2851–2856
35. Campanacci, V., Krieger, J., Bette, S., Sturgis, J.N., Lartigue, A., Cambillau, C., Breer, H., and Tegoni, M. (2001) Revisiting the specificity of *Mamestra brassicae* and *Antheraea polyphemus* pheromone-binding proteins with a fluorescence assay. *J. Biol. Chem.* **276**, 20078–20084
36. Bette, S., Breer, H., and Krieger, J. (2002) Probing a pheromone binding protein of the silkmoth *Antheraea polyphemus* by endogenous tryptophan fluorescence. *Insect Biochem. Mol. Biol.* **32**, 241–246
37. Kitabayashi, A., Arai, T., Kubo, T., and Natori, S. (1998) Molecular cloning of cDNA for p10, a novel protein that increases in the regenerating legs of *Periplaneta americana* (American cockroach). *Insect Biochem. Mol. Biol.* **28**, 785–790
38. Sabatier, L., Jouanguy, E., Dostert, C., Zachary, D., Dimarcq, J., Bulet, P., and Imler, J. (2003) Pherokine-2 and -3. *Eur. J. Biochem.* **270**, 3398–3407
39. Bohbot, J., Sobrio, R., Lucas, R., and Nagnan-Le Meillour, P. (1998) Functional characterization of a new class of odorant-binding proteins in the moth *Mamestra hrassicae*. *Biochem. Biophys. Res. Commun.* **253**, 489–494
40. Ozaki, M., Wada-Katsumata, A., Fujikawa, K., Iwasaki, M., Yokohari, F., Satoji, Y., Nisimura, T., and Yamaoka, R. (2005) Ant nestmate and non-nestmate discrimination by a chemosensory sensillum. *Science* **309**, 311–314
41. Zhang, Z.C., Wang, M.Q., Lu, Y.B., and Zhang, G.A. (2009) Molecular characterization and expression pattern of two general odorant binding proteins from

the diamondback moth, *Plutella xylostella*. *J. Chem. Ecol.* **35**, 1188–1196
42. Reddy, G.V.P. and Guerrero, A. (2000) Behavioral responses of the diamondback moth, *Plutella xylostella*, to green leaf volatiles of *Brassica oleracea* subsp. *Capitata*. *J. Agric. Food Chem.* **48**, 6025–6029
43. Wanner, K.W., Isman, M.B., Feng, Q., Plettner, E., and Theilmann, D.A. (2005) Developmental expression patterns of four chemosensory protein genes from the eastern spruce budworm, *Chroistoneura fumiferana*. *Insect Mol. Biol.* **14**, 289–300
44. Nomura, A., Kawasaki, K., Kubo, T., and Natori, S. (1992) Purification and localization of p10, a novel protein that increases in nymphal regenerating legs of *Periplaneta americana* (American cockroach). *Int. J. Dev. Biol.* **36**, 391–398
45. Tulik, G.R., Chodavarapu, S., Edgar, R., Giannunzio, L., Langland, A., Schultz, B., and Beckmann, J.D. (2002) Inhibition of bovine phenol sulfotransferase (bSULT1A1) by CoA thioesters. Evidence for positive cooperativity and inhibition by interaction with both the nucleotide and phenol binding sites. *J. Biol. Chem.* **277**, 39296–39303
46. Lartigue, A., Campanacci, V., Roussel, A., Larsson, A.M., Jones, T.A., Tegoni, M., and Cambillau, C. (2002) X-ray structure and ligand binding study of a moth chemosensory protein. *J. Biol. Chem.* **277**, 32094–32098
47. Picimbon, J.F. (2003) Biochemistry and evolution of OBP and CSP proteins (Blomquist, G.J. and Vogt, R.G., eds.), pp. 539–566, Elsevier Academic Press, London
48. Xiu, W.M., Zhou, Y.Z., and Dong, S.L. (2008) Molecular characterization and expression pattern of two pheromone-binding proteins from *Spodoptera litura* (Fabricius). *J. Chem. Ecol.* **34**, 487–498